Cancer Imaging (2012) **12,** 31–40
DOI: 10.1102/1470-7330.2012.0005

CI

e-med
www.e-med.org.uk

ORIGINAL ARTICLE

CT-based quantitative SPECT for the radionuclide ^{201}Tl: experimental validation and a standardized uptake value for brain tumour patients

Kathy Willowson[a,b], Dale Bailey[a,b,c], Geoff Schembri[b] and Clive Baldock[a]

[a]Institute of Medical Physics, School of Physics, University of Sydney, Camperdown, NSW 2006, Australia; [b]Department of Nuclear Medicine, Royal North Shore Hospital, St Leonards, NSW 2065, Australia; [c]Discipline of Medical Radiation Sciences and Sydney Medical School, Faculties of Health, University of Sydney, Lidcombe, NSW 2141, Australia

Corresponding address: Dr Kathy Willowson, Department of Nuclear Medicine, Royal North Shore Hospital, St Leonards, NSW 2065, Australia.
Email: k.willowson@physics.usyd.edu.au

Date accepted for publication 1 December 2011

Abstract

We have previously reported on a method for reconstructing quantitative data from ^{99m}Tc single photon emission computed tomography (SPECT) images based on corrections derived from X-ray computed tomography, producing accurate results in both experimental and clinical studies. This has been extended for use with the radionuclide ^{201}Tl. Accuracy was evaluated with experimental phantom studies, including corrections for partial volume effects where necessary. The quantitative technique was used to derive standardized uptake values (SUVs) for ^{201}Tl evaluation of brain tumours. A preliminary study was performed on 26 patients using ^{201}Tl SPECT scans to assess residual tumour after surgery and then to monitor response to treatment, with a follow-up time of 18 months. Measures of SUV_{max} were made following quantitative processing of the data and using a threshold grown volume of interest around the tumour. Phantom studies resulted in the calculation of concentration values consistently within 4% of true values. No continuous relation was found between SUV_{max} (post-resection) and patient survival. Choosing an SUV_{max} cut-off of 1.5 demonstrated a difference in survival between the 2 groups of patients after surgery. Patients with an $SUV_{max} < 1.5$ had a 70% survival rate over the first 10 months, compared with a 47% survival rate for those with $SUV_{max} > 1.5$. This difference did not achieve significance, most likely due to the small study numbers. By 18 months follow-up this difference had reduced, with corresponding survival rates of 40% and 27%, respectively. Although this study involves only a small cohort, it has succeeded in demonstrating the possibility of an SUV measure for SPECT to help monitor response to treatment of brain tumours and predict survival.

Keywords: *SPECT; single photon emission computed tomography; standardized uptake value; brain; thallium-201.*

Introduction

The benefits of acquiring quantitative data in nuclear diagnostic and therapeutic studies are widely recognized and have been utilized in an extensive range of applications[1–6]. Limitations involved in quantitative accuracy stem from the ability to provide practical and effective corrections for photon interactions that occur in the body due to attenuation and scatter, and to take into account camera-specific properties and clinical difficulties such as patient motion. Although quantitative positron emission tomography (PET) has become a standard clinical technique to aid in the diagnosis of disease and monitoring of patient response to treatment, quantitative single photon emission computed tomography (SPECT) has not. Recent growth in the area of quantitative SPECT can be largely attributed to the introduction of combined SPECT/CT systems[3,7,8], allowing the high-resolution transmission data provided by X-ray computed tomography (CT) to be used not only in image

This paper is available online at http://www.cancerimaging.org. In the event of a change in the URL address, please use the DOI provided to locate the paper.

fusion for anatomic correlation, but for patient-specific non-uniform attenuation and scatter correction.

The authors have previously developed a method for producing fully quantitative ^{99m}Tc SPECT images based on corrections derived from X-ray CT data[9,10] for attenuation and scattering of photons, which, when combined with corrections for camera dead time, partial volume effects and camera sensitivity, produce consistently accurate results in both experimental and clinical data. Following on from this work, the aim was to extend the CT-based quantitative technique to include other clinically useful radionuclides. In particular, the radionuclide ^{201}Tl was investigated due to its application in imaging of brain tumours.

The role of ^{201}Tl SPECT imaging in patients with brain tumours has been explored in numerous publications. ^{201}Tl uptake is considered to be multifactorial relating to the Na–K ATPase system, tumour vascularity, cellular membrane permeability and tumour viability[11,12]. In brain tumours, ^{201}Tl uptake may additionally be related to regional cerebral blood flow and blood–brain barrier breakdown as thallium does not cross an intact blood-brain barrier[13,14].

Several reports have assessed ^{201}Tl SPECT scintigraphy in the grading of gliomas[15–22] and the differentiation of primary brain tumours from other lesions[23,24].

Discriminating between residual or recurrent viable tumour from post-therapeutic changes such as radiation necrosis has also been extensively studied. As early as 1991[25] thallium uptake was demonstrated to correlate with tumour recurrence. Others have assessed this further by tumour to scalp ratios[26], tumour to normal brain ratios[14,27–31] tumour to myocardial uptake[32], retention rates on delayed imaging[14,31] and visual inspection[33,34].

Determining prognosis has also been assessed. A semi-quantitative approach to predict overall survival of patients with brain tumours was carried out by Vos et al.[35]. The research aimed at introducing SPECT and magnetic resonance imaging (MRI)/CT cut-off values that could provide a diagnostic classification and predict overall survival at the early stages of treatment. Images had no scatter or attenuation correction, and the scale was based on the ratio of maximum uptake in the tumour to background. Whilst such a method is not quantitative, it was found that, on the basis of two ^{201}Tl SPECT scans (early and delayed), predictions could be made regarding expected survival of patients with the aim of selective aggressive treatment. Similarly, Comte et al.[36] found significant correlation between pre-operative ^{201}Tl SPECT with histologic grading and overall survival of patients with glioma. The recent publication by Iida[31] suggested that early uptake is the best predictor of progression-free survival. In 2011, Vos et al.[37] reported a strong correlation between survival and the tumour to normal brain ratio. Similar findings have been reported by others[33,38–40].

Although anatomic imaging is highly sensitive when imaging the brain, its specificity is lacking, such that CT or MRI alone are limited in their evaluation of patients with brain tumours[41,42]. In addition, such modalities also show interobserver variability[43], a limitation that could be overcome if fully quantitative evaluation from functional images were to be made available.

Other studies have reported no correlation between uptake and tumour type or survival for certain types of brain tumour, in particular, pilocytic astrocytoma and oligodendroglioma[36,44]. Furthermore, some groups have disagreed with such a correlation altogether, and argued for the superiority of CT or MRI[45,46]. The literature suggests that a fully quantitative evaluation of ^{201}Tl SPECT may have a role to play, particularly for objective analysis of such data.

In PET studies, quantitative analysis is carried out with the aid of the standardized uptake value (SUV)[47]. This dimensionless quantity is calculated from the measured concentration of activity in the lesion or region of interest, and the total injected dose in the patient of a specified weight, and is defined as

$$\mathrm{SUV} = \frac{\mathrm{kBq\,ml^{-1}\ (tumour)}}{\mathrm{dose\,(kBq)/weight\,(g)}} \quad (1)$$

Due to the lack of fully quantitative SPECT in routine clinical practice, the potential for SUVs in SPECT imaging of cancer has not been widely recognized. A recent investigation by Beauregard et al.[48] successfully demonstrated the application of SUV measures in imaging of neuroendocrine tumours after ^{177}Lu therapy, indicating the potential usefulness of such a measure for tumour analysis and treatment monitoring. Despite the role of SPECT in brain imaging, the authors are unaware of an equivalent measure for SPECT analysis of brain tumours.

Specifically, this work aims to develop and validate a CT-based quantitative technique for ^{201}Tl SPECT, and to investigate the feasibility of a applying such a technique to ^{201}Tl brain tumour studies with the aim of developing an SUV.

Materials and methods

All experimental and clinical data were acquired with a triple-head Picker Prism 3000XP SPECT system (Picker, Cleveland, OH, USA) of crystal thickness 9.5 mm, with low-energy high-resolution (LEHR) collimators of hole size 1.40 mm, hole length 27.0 mm, septal thickness 0.18 mm, 8.0 mm system full-width-at-half-maximum (FWHM) at 10 cm, and a 240×400 mm field of view. The corresponding CT data were acquired on a single-slice Picker PQ5000 helical CT scanner[49]. Emission data were acquired using an energy window spanning 60–90 keV. The protocol for brain imaging consisted of a 30-min SPECT study of 120 projections (45 s per projection angle), acquired on a 128 by 128 matrix size with

a zoom of 1.0, resulting in final voxel dimensions of 3.56 mm. All reconstruction was performed using OSEM (ordered subset expectation maximization) with 4 iterations and 8 subsets, followed by three-dimensional Butterworth filtering with a cut-off of 1.0 and order of 8.0. All analysis was performed on a HERMES workstation (Nuclear Diagnostics AB, Stockholm) and software written in IDL (ITT, Boulder, CO).

Experimental measures

Following the methodology described previously in Willowson et al.[9], the quantitative method required CT-based corrections for scatter and attenuation, combined with measurements of the camera sensitivity factor and modelling of the partial volume effect. Briefly, the transmission-dependent scatter correction (TDSC) method, originally described by Meikle et al.[50], was used to perform object-specific, non-uniform scatter correction, based on radionuclide, camera and collimator specific measures of the scatter function and scatter fraction (k), given by

$$k = 1 - \frac{1}{A - B(\mathrm{e}^{-\mu T})^{\beta/2}} \quad (2)$$

where $\mathrm{e}^{-\mu T}$ represents the transmission factor at a point for a given object thickness T, and can hence be calculated from X-ray CT data using the known relationship between Hounsfield units and linear attenuation coefficients[51], and provided the empirical parameters A, B and β are known. The scatter function represents the response of a position-sensitive detector to scattered radiation, which cannot be discriminated from the photopeak due to the limited energy resolution of the camera. Standard evaluation is from line source experiments, modelling scatter tails in the count profile as decreasing mono-exponentials[52].

Experimental measures of the scatter function slope and scatter fraction parameters A, B and β were made through line source and build-up experiments, respectively.

Following the technique described previously in Willowson et al.[9], a low activity source with negligible attenuation and scatter was imaged, and the background subtracted average count rate per detector compared with the calibrated activity to derive the sensitivity factor in units of count s^{-1} MBq^{-1}. Partial volume effects were modelled using cylinders of varying diameter (ranging from approximately 0.5 to 10 times the system spatial resolution). Comparison of the true concentration within the objects with the measured concentration from corrected images led to calculated recovery coefficients. A function of the form

$$y = 1 - a(e^{-bx}) \quad (3)$$

was fitted to the data to allow for easy calculation of recovery coefficient values (y) for a given object diameter (x).

The reconstructed spatial resolution of the system was evaluated through the FWHM of a profile representing counts across the reconstructed SPECT study of a line source.

The CT-based quantitative method

The quantitative algorithm described in Willowson et al.[9] was modified to include the radionuclide specific parameters corresponding to the experimental results for ^{201}Tl. The quantitative method first involved conversion of the CT data into an energy-dependent linear attenuation map, or μ-map[51]. For ^{201}Tl, the average energy of the X-ray spectrum was used for this conversion, resulting in an attenuation coefficient of 0.16 cm^{-1}.

The μ-map provided information of attenuation at every point in the observed image ($g(x,y)_{obs}$), which was used to calculate a matrix of scatter fraction values ($k(x,y)$) based on the measured TDSC parameters and Eq. (2). When combined with the measured scatter function (s), this allowed for a non-uniform, patient-specific estimate of scatter that could be subtracted to leave scatter-free projection data ($g(x,y)$):

$$g(x,y) = g(x,y)_{obs} - k(x,y)(g(x,y)_{obs} \otimes s \quad (4)$$

This scatter-corrected data was then corrected for attenuation, again using the CT-derived μ-map and an iterative Chang attenuation correction algorithm[53], resulting in fully corrected reconstructed slices. The measured camera sensitivity factor allowed for conversion of the corrected reconstructions into units of absolute activity, after which any relevant partial volume effects could be taken into account by using the known object size (measured from the CT data) and the corresponding recovery coefficient. No camera dead time effects were modelled as, considering typical clinical doses associated with ^{201}Tl, these were assumed to be negligible.

Experimental validation

A cylindrical phantom containing a range of fixed attenuating materials (made from Styrofoam, epoxy and sand) of diameter 20 cm and volume 4810 ml was used to provide an initial validation of the technique. The phantom was filled with a calibrated amount of radioactivity mixed uniformly in water, giving a known concentration of 21 kBq ml^{-1}. SPECT/CT was performed. The emission data were reconstructed following the quantitative method described above, and the mean calculated concentration of radioactivity found in hand-drawn regions of interest (ROIs) over several slices in background was compared with the known amount.

Further quantitative validation was performed using an RSD anthropomorphic striatal brain phantom (Radiology Support Devices, Elimpex-Medizintechnik, Austria). The brain phantom is made from Perspex and contains 4 compartments situated inside the main cerebral cavity (volume of 1260 ml), representing the

subcortical grey matter regions, or striatum, of the brain (specifically the caudate nuclei and putamen bilaterally; volumes 5.4 ml and 6.0 ml, respectively). Each of these compartments could be accessed separately from the main volume, allowing different concentrations of radioactivity to be used in each. The phantom itself was housed in a replica skull made from materials that strongly resemble the density, and hence attenuation and scattering properties, of human bone and flesh, allowing for a realistic emulation of the clinical situation.

For quantitative validation, the background cavity was filled with water and a uniform concentration of 40.2 kBq ml^{-1} of ^{201}Tl. One of the 4 compartments was left cold with no radioactivity (water with 0 kBq ml^{-1}); the other 3 compartments were filled with increasing concentrations of solutions, in the ratios of 2.5, 4, and 5 times that of the background. These concentrations were calibrated as 109 kBq ml^{-1}, 164 kBq ml^{-1} and 218 kBq ml^{-1} at mid-scan time. The phantom was sealed inside the skull and SPECT data acquired on the Picker Prism 3000XP gamma camera, following the standard 30-min acquisition protocol described above. An X-ray CT was also acquired at the time of the study and used to perform quantitative corrections on the data. The calculated concentrations of activity in the lesions and in the background were compared with the known concentrations to evaluate the accuracy of the quantitative method. This evaluation also required application of the appropriate recovery coefficients to the values recovered from the lesions due to the partial volume effects on their small sizes. ROIs were drawn based on the true contour of the lesions using the CT data.

Clinical investigation: SUV measures in brain tumour studies

A quantitative investigation of the data from a clinical study between the Department of Nuclear Medicine and Radiation Oncology at Royal North Shore Hospital, Sydney, was used to assess the possibility of introducing an SUV measure to ^{201}Tl brain SPECT in patients undergoing treatment for malignant brain tumours. The time of camera calibration and quantitative testing took place toward the end of, but during, the period of patient imaging.

The study involved 27 patients (17 males, 10 females) who were recruited over the period 2005–2008, 20 of whom were deceased at final follow-up (late 2009) and one of whom refused treatment and so was withdrawn from the study. Patients were in the age range of 27–83 years, with a mean age of 61.3 years. All patients participating in the study had been diagnosed with a form of brain malignancy, predominantly astrocytoma, and were undergoing treatment through surgical resection or debulking, radiotherapy, and chemotherapy. All patients had a ^{201}Tl SPECT study performed in the first week after surgery to assess remnant tumour and treatment options. The study consisted of imaging 15 min after injection of approximately 120 MBq of thallium chloride (^{201}Tl) using the triple-headed Picker Prism 3000XP gamma camera following the protocol mentioned above (the same as that used in the experimental investigations). The co-registered radiation therapy planning CT was used for all quantitative corrections. Delayed imaging was optional and was performed on 8 patients. Of the initial 27 patients, 12 returned for a follow-up study 3 months after surgery, and 4 returned for a follow-up study 6 months after surgery (follow-up SPECT data are not presented in this report). X-ray CT and MRI were performed on all patients routinely to assess recurrence and post-operative change, and all studies aided in monitoring treatment.

Data were first reconstructed with no corrections and, following the standard method of analysis, the ratio of maximum counts inside a hand-drawn region over the tumour to a similar size region drawn over healthy brain was recorded. Generally speaking, such a tumour-to-background ratio above 1.0 is considered to be an indicator of recurrent disease. The higher such a ratio, the more likely recurrence, and the more aggressive the treatment needed.

For the purposes of this study, all SPECT data were corrected using the CT-based quantitative method described above, producing images in units of kBq ml^{-1}. To determine SUVs, volumes of interest were drawn around the tumour using a volume growing package[54], based on a specified threshold of the maximum pixel value within the tumour. The maximum concentration value within each tumour volume was recorded and used to generate SUV_{max} values using Eq. (1), which were compared with patient survival (in terms of months from the initial SPECT study) and analysed via linear regression. Maximum concentration was chosen to measure the SUV due to asymmetric tumour shapes and the associated difficulty in measuring consistent tumour diameters in order to apply a suitable recovery coefficient factor. In patients who had multiple foci, the largest value was chosen. An arbitrary SUV_{max} cut-off of 1.5 was chosen to compare relative survival of patients both above and below this threshold over an 18 month follow-up time using Kaplan–Meier analysis and a log-rank test. The cut-off was chosen based on good separation of the group's survival. In the subgroup on whom 4-h delayed imaging was obtained ($n = 8$), comparison of tumour-to-background ratio and SUV_{max} on delayed and early imaging was performed. Several studies were also chosen randomly to be used for normal background calculations. An ROI was drawn in areas of normal brain, contralateral to the tumour site, and the average across all studies taken as an indicator of SUV in healthy brain. All ROIs and volumes of interest were drawn by a nuclear medicine physician with the aid of co-registered MRI/CT images to differentiate between uptake in the brain and skull where necessary.

Results

Experimental measurements

Table 1 contains the resulting parameters found for ^{201}Tl. Results displayed in Table 1 are: the measured slope of the mono-exponential function used to model the scatter function; the empirical parameters that describe the scatter fraction (A, B, β); the measured camera sensitivity factor; and the reconstructed spatial resolution.

Figure 1 demonstrates the measured scatter fraction modelled with the build-up function (Eq. (2)). Fig. 2 represents the resulting recovery coefficient plot for ^{201}Tl, with Eq. (3) fitted to the data. The plot is as expected with true concentrations being recovered only when object diameters reach ~4 times the system spatial resolution.

Table 1 Experimental measures for ^{201}Tl of the slope of the scatter function (s), the scatter fraction parameters (A, B and β) that describe the build-up function, the measured camera sensitivity factor, and the reconstructed system spatial resolution to be used in conjunction with the measured recovery coefficients for partial volume corrections

Experimental parameter	Measured value
Scatter function s (cm^{-1})	0.28 ± 0.2
Scatter fraction	
A	2.89 ± 0.31
B	1.88 ± 0.31
β	0.25 ± 0.05
Sensitivity (counts s^{-1} MBq^{-1})	126.7 ± 1.3
Spatial resolution (mm)	19.8 ± 0.2

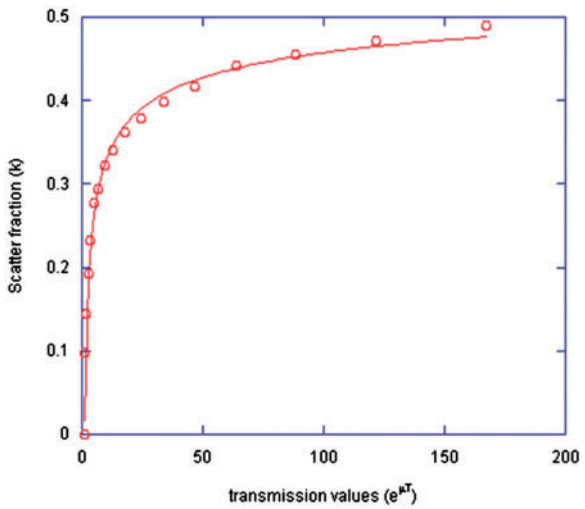

Figure 1 **The measured scatter fraction values for increasing thickness of scattering medium when imaging ^{201}Tl, modelled with the build-up function (Eq. (2)).**

Quantitative validation

The cylindrical phantom was known to contain a concentration of ^{201}Tl equal to 21 kBq ml^{-1} at the time of the study. Taking the average measured concentration from several ROIs across several transverse slices, the quantitative method led to a calculated concentration within 1% of the true value.

Table 2 summarizes the results of the quantitative analysis of the RSD anthropomorphic striatal brain phantom. In Table 2, the true concentrations of activity in each of the lesions and the background compartment are compared with the calculated concentrations, both with and without corrections for the partial volume effect. The calculated recovery coefficient for each volume is also listed, as is the difference between the final corrected concentration values and true values.

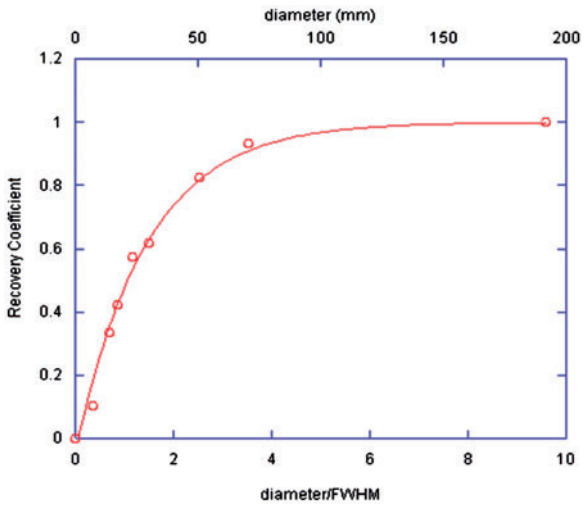

Figure 2 **Recovery coefficient values for each object size against the diameter as a fraction of the system spatial resolution (FWHM).**

Table 2 Quantitative validation using the RSD anthropomorphic striatal brain phantom

Region	True kBq ml^{-1}	Measured kBq ml^{-1}	Recovery coefficient	Calculated kBq ml^{-1}	Difference (%)
Background	40.2	41.1	–	41.1	+2.2
Cold lesion	0	26.5	–	–	–
Lesion 1	109	52.6	0.5	105.2	−3.5
Lesion 2	164	79.2	0.5	158.4	−3.4
Lesion 3	218	110.1	0.5	220.0	+0.9

The true activity concentrations are compared with calculated mean concentrations both with and without corrections for partial volume effects, for the background and lesions of varying activity ratios. The differences between the true and calculated concentrations, when all corrections are taken into account, are displayed as a percentage of the true values.

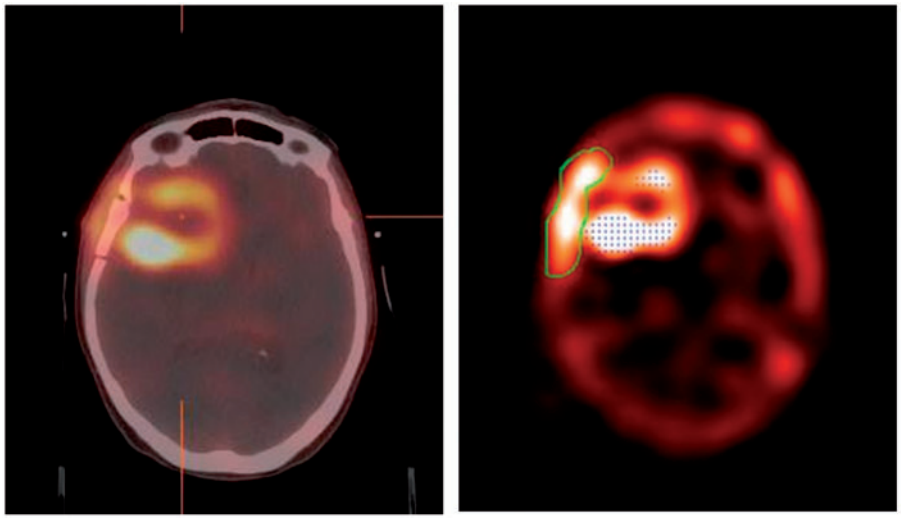

Figure 3 **Example of a reconstructed quantitative ^{201}Tl SPECT with a Butterworth filter, co-registered to the radiotherapy treatment planning CT (left), and the corresponding threshold grown ROI (right).**

Clinical investigation

Fig. 3 represents a reconstructed SPECT study, co-registered to the radiotherapy treatment planning CT, and the corresponding threshold-based region-growing software analysis for the same patient. Fig. 4(a,b) represents the observed relationship between SUV_{max} (early imaging only) with survival of patients with a brain tumour and measured tumour-to-background ratios, respectively. A direct comparison of tumour-to-background ratio and survival can be seen in Fig. 4(c). Linear regression analysis yields a poor relation between SUV_{max} and survival, with no significant correlation found between the two based on a log-rank test. The relationship between SUV_{max} and tumour-to-background ratio can be described as linear, with a correlation coefficient equal to 0.6, and as significant ($P < 0.005$).

In SPECT studies performed post-surgery (pre-therapy), tumour-to-background ratios were found to range from 1 (normal) to 8, with a mean of 2.7. The maximum concentration within tumours, using the CT-based quantitative method, ranged from 0.5 kBq ml^{-1} to 7.8 kBq ml^{-1}, with a mean of 3.2 kBq ml^{-1}, with corresponding SUV_{max} values ranging from 0.4 to 4.6, with a mean of 2.0.

Table 3 displays the differences seen between early and delayed imaging in tumour-to-background ratios and SUV_{max} values.

Relative survival of patients both above and below an SUV_{max} threshold of 1.5 were compared over an 18-month follow-up time. Fig. 5 demonstrates the relative fraction of patients surviving over this time period in each of the 2 groups. At 10 months after surgery, patients with an $SUV_{max} < 1.5$ demonstrated a 70% survival, compared with 47% survival for those with an $SUV_{max} > 1.5$. At 18 months after surgery, these survival rates had fallen to 40% and 27%, respectively. A log-rank test demonstrated no significant difference in survival rates between the 2 groups ($P > 0.2$).

Although no significant correlation between SUV_{max} and survival was seen over the entire range of patients, examination of those who fell at the extreme ends of the spectrum demonstrates a significant correlation ($P = 0.005$). Those with an initial $SUV_{max} < 1.0$ (7 patients) were found to have an average survival time of 16.4 months (range 8–24 months); those with $SUV_{max} > 3.5$ (4 patients) had an average survival of only 3.8 months (range 2–9 months).

Discussion

Accurate modelling of the scatter correction parameters and experimental measurement for sensitivity are indicated by close agreement between the measured and true concentrations in the cylindrical phantom experiment. These results are consistent with the RSD anthropomorphic striatal brain phantom experiment, where measured concentrations in all lesions and background were within 4% of the true values. In addition, the brain phantom study also suggests correct modelling of the partial volume effect, and allows for an evaluation of quantitative accuracy for a range of tumour-to-background activity ratios, representative of clinical imaging. It is unlikely that the measured experimental correction parameters would fluctuate much over an extended period of time unless the camera underwent installation of new hardware/software, or was damaged. The most susceptible measure is the sensitivity factor, which may require repeated measurements over extended periods of time (years).

When considering the cold lesion, although the volume of the lesion contained no radioactivity, a measured concentration of 26.5 kBq ml^{-1} was found. This erroneous

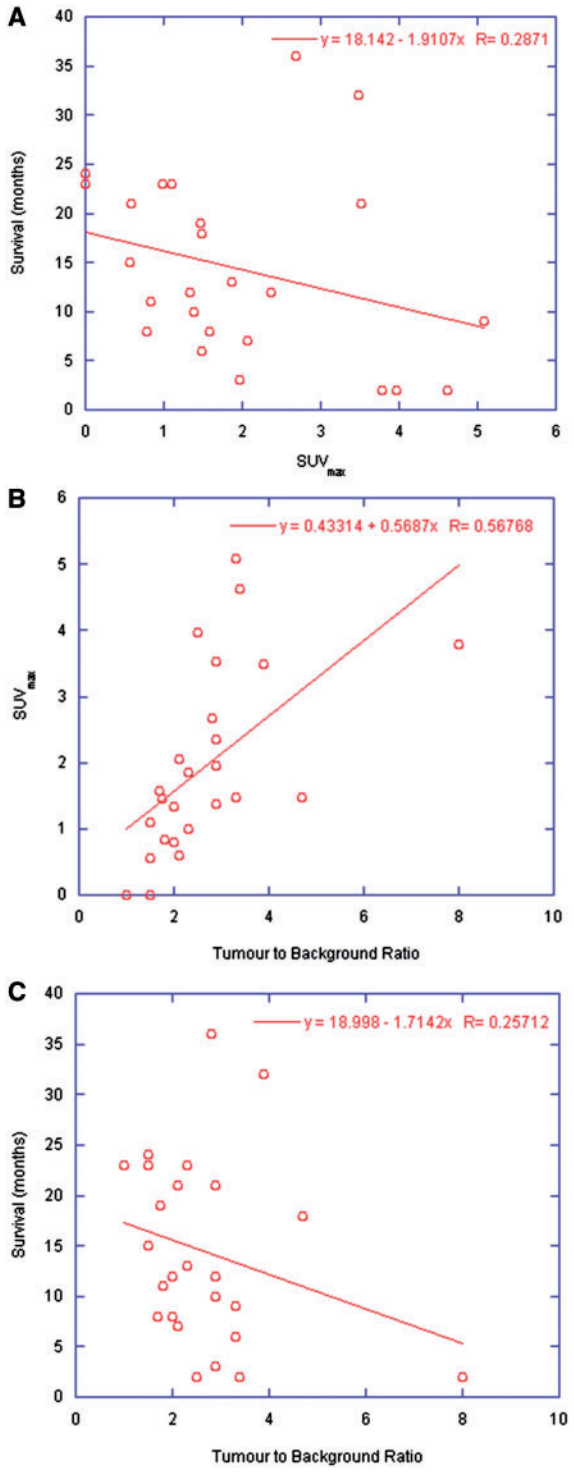

Figure 4 **Relationship between (a) baseline SUV_{max} and survival, (b) baseline SUV_{max} and measured tumour-to-background ratio, and (c) tumour-to-background ratio and survival.**

measurement is due to spillover from outside the volume and scatter, and considering the small size of the lesion and its position within the background activity and immediately adjacent to a hot lesion, this result is not unexpected.

Table 3 Relative changes in tumour-to-background ratios (T:B) and SUV_{max} values between initial and delayed imaging as measured on 8 patient studies

Patient	$\Delta T{:}B$ (%)	ΔSUV_{max} (%)
1	−25.0	−2.9
2	−28.6	31.0
3	−5.9	33.2
4	−17.9	16.9
5	−13.3	0.0
6	−20.0	0.0
7	−8.7	17.9
8	0.0	61.8
Mean ± SD	−14.9 ± 9.8	19.7 ± 22.0

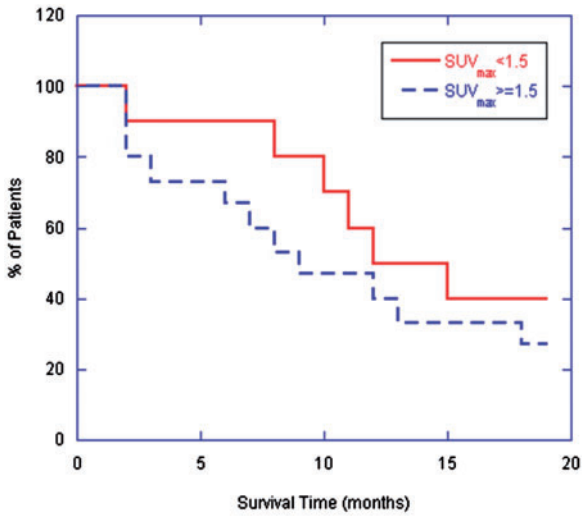

Figure 5 **Fraction of surviving patients over initial 18 months post-SPECT categorized by the arbitrary cut-off of baseline SUV_{max} equal to 1.5.**

The phantom results are indicative of a robust quantitative method for analysis of ^{201}Tl SPECT data that should extend to clinical imaging. The patient studies analysed as part of this research are meant as a pilot study to test the feasibility of such a method. It is important to note that treatment was not consistent across all patients, and a larger cohort is necessary to draw conclusions. However, some initial insights have been gained from this study.

Of the 8 patients who underwent delayed (4 h) SPECT imaging, the mean change in tumour-to-background ratio and SUV_{max} was 14.9% and 19.7%, with a range of (0–28.6)% and (0–61.8)%, respectively. The rationale behind such delayed imaging is that ^{201}Tl does exhibit some uptake in post-surgical oedema, which decreases with time, whereas tumour uptake is expected to decrease more slowly or even increase, hence delayed imaging can help to differentiate between recurrence and post-surgical change. Some patients did display large relative changes

between early and delayed measures, however a larger patient cohort is necessary to determine whether or not this may be significant.

In comparison with previous studies in the literature[35,36,55], no significant or linear correlation was found between tumour-to-background ratio and survival, however such statistical analysis is most likely limited by the small study cohort. Furthermore, although very low or very high SUVs appear to correlate with survival, greater study numbers are needed to support this.

Given the relatively poor survival times associated with patients with brain tumours and the limited study numbers, it is difficult to draw conclusions regarding the impact that quantitative analysis may have on the management of such patients. Given the lack of correlation between the standard method of analysis (tumour-to-background ratio) or quantitative analysis with survival, the study does not indicate that ^{201}Tl SPECT has added anything significant to prognostication for these patients. However, the impact that such a method may have on guiding radiotherapy planning is still open to investigation. Furthermore, given the correlation that has been demonstrated in the literature between tumour-to-background ratios with survival, this would again suggest that larger numbers are needed before conclusions can be drawn.

It is likely be that the role of thallium imaging in brain tumours will be more in the areas of assisting with radiotherapy planning and for differentiating between radiation necrosis and recurrence rather than initial post-operative assessment.

Conclusion

A practical method for achieving fully quantitative SPECT data for the radionuclide ^{201}Tl has been developed and validated on experimental data. The method is based on a previously developed technique for achieving quantitative ^{99m}Tc SPECT data, and uses the transmission information available from co-registered CT data to perform non-uniform, patient-specific corrections for scatter and attenuation, with the additional benefit of having the high-resolution CT data available for image fusion and measurement of object size when partial volume effect corrections are necessary. As such, the method is ideal for use on clinical SPECT/CT systems, and has been found to produce consistent results.

Initial results from a small pilot study to investigate the feasibility of an SUV parameter for brain SPECT imaging have demonstrated trends in survival of patients with initial SUV_{max} values above or below 1.5, and has suggested SUV may be able to indicate survival for patients who fall at the extreme ends of the spectrum (a very large (>3.5) or very low (<1.0) SUV). Incorporating the CT-based quantitative method into the analysis of ^{201}Tl brain SPECT studies to derive fully quantitative SUV parameters has been demonstrated and, given the role that SUV has played in PET, we would expect this to present new opportunities for SPECT in the analysis and monitoring of disease.

References

[1] Groshar D, Frankel A, Iosilevsky G, *et al.* Quantitation of renal uptake of technetium-99m DMSA using SPECT. J Nucl Med 1989; 30: 246–50.

[2] Zasadny KR, Wahl RL. Standardized uptake values of normal tissues at PET with 2-[fluorine-18]-fluoro-2-deoxy-D-glucose: variations with body weight and a method for correction. Radiology 1993; 189: 847–50.

[3] Grossman GB, Garcia EV, Bateman TM, *et al.* Quantitative Tc-99m sestamibi attenuation-corrected SPECT: development and multicenter trial validation of myocardial perfusion stress gender-independent normal database in an obese population. J Nucl Cardiol 2004; 11: 263–72. doi:10.1016/j.nuclcard.2004.02.007.

[4] Bailey DL, Willowson KP, Timmin S, Harris BE, Bailey EA, Roach PJ. Quantitative pre-surgical lung function estimation with SPECT/CT. ANZ Nucl Med J 2009; 40: 5–7.

[5] Thiele F, Ehmer J, Piroth MD, *et al.* The quantification of dynamic FET PET imaging and correlation with the clinical outcome in patients with glioblastoma. Phys Med Biol 2009; 54: 5525–39. doi:10.1088/0031-9155/54/18/012.

[6] Willowson K, Bailey DL, Baldock C. Quantifying lung shunting during planning for radio-embolization. Phys Med Biol 2011; 56: N145–52. doi:10.1088/0031-9155/56/13/N01.

[7] Larsson A, Johansson L, Sundstrom T, Ahlstrom KR. A method for attenuation and scatter correction of brain SPECT based on computed tomography images. Nucl Med Commun 2003; 24: 411–20. doi:10.1097/00006231-200304000-00011.

[8] Shcherbinin S, Celler A, Belhocine T, Vanderwerf R, Driedger A. Accuracy of quantitative reconstructions in SPECT/CT imaging. Phys Med Biol 2008; 53: 4595–604. doi:10.1088/0031-9155/53/17/009.

[9] Willowson K, Bailey DL, Baldock C. Quantitative SPECT reconstruction using CT-derived corrections. Phys Med Biol 2008; 53: 3099–112. doi:10.1088/0031-9155/53/12/002.

[10] Willowson K, Bailey DL, Bailey EA, Baldock C, Roach PJ. In vivo validation of quantitative SPECT in the heart. Clin Physiol Funct Imaging 2010; 30: 214–9. doi:10.1111/j.1475-097X.2010.00930.x.

[11] Brismar T, Collins VP, Kesselberg M. Thallium-201 uptake relates to membrane potential and potassium permeability in human glioma cells. Brain Res 1989; 500: 30–6. doi:10.1016/0006-8993(89)90296-5.

[12] Pauwels EK, McCready VR, Stoot JH, van Deurzen DF. The mechanism of accumulation of tumour-localising radiopharmaceuticals. Eur J Nucl Med 1998; 25: 277–305. doi:10.1007/s002590050229.

[13] Benard F, Romsa J, Hustinx R. Imaging gliomas with positron emission tomography and single-photon emission computed tomography. Semin Nucl Med 2003; 33: 148–62. doi:10.1053/snuc.2003.127304.

[14] Sun D, Liu Q, Liu W, Hu W. Clinical application of ^{201}Tl SPECT imaging of brain tumors. J Nucl Med 2000; 41: 5–10.

[15] Burkard R, Kaiser KP, Wieler H, *et al.* Contribution of thallium-201-SPECT to the grading of tumorous alterations of the brain. Neurosurg Rev 1992; 15: 265–73.

[16] Oriuchi N, Tamura M, Shibazaki T, *et al.* Clinical evaluation of thallium-201 SPECT in supratentorial gliomas: relationship to histologic grade, prognosis and proliferative activities. J Nucl Med 1993; 34: 2085–9.

[17] Kallen K, Heiling M, Andersson AM, Brun A, Holtas S, Ryding E. Preoperative grading of glioma malignancy with

thallium-201 single-photon emission CT: comparison with conventional CT. AJNR Am J Neuroradiol 1996; 17: 925–32.
[18] Lam WW, Chan KW, Wong WL, Poon WS, Metreweli C. Preoperative grading of intracranial glioma. Acta Radiol 2001; 42: 548–54. doi:10.1034/j.1600-0455.2001.420603.x.
[19] Comte F, Bauchet L, Rigau V, *et al.* Correlation of preoperative thallium SPECT with histological grading and overall survival in adult gliomas. Nucl Med Commun 2006; 27: 137–42. doi:10.1097/01.mnm.0000191855.19327.af.
[20] Black KL, Hawkins RA, Kim KT, Becker DP, Lerner C, Marciano D. Use of thallium-201 SPECT to quantitate malignancy grade of gliomas. J Neurosurg 1989; 71: 342–6. doi: 10.3171/jns.1989.71.3.0342.
[21] Sjoholm H, Elmqvist D, Rehncrona S, Rosen I, Salford LG. SPECT imaging of gliomas with thallium-201 and technetium-99m-HMPAO. Acta Neurol Scand 1995; 91: 66–70. doi:10.1111/j.1600-0404.1995.tb05846.x.
[22] Tamura M, Shibasaki T, Zama A, *et al.* Assessment of malignancy of glioma by positron emission tomography with ^{18}F-fluorodeoxyglucose and single photon emission computed tomography with thallium-201 chloride. Neuroradiology 1998; 40: 210–5. doi:10.1007/s002340050569.
[23] Kojima Y, Kuwana N, Noji M, Tosa J. Differentiation of malignant glioma and metastatic brain tumor by thallium-201 single photon emission computed tomography. Neurol Med Chir (Tokyo) 1994; 34: 588–92. doi:10.2176/nmc.34.588.
[24] Kallen K, Heiling M, Andersson AM, Brun A, Holtas S, Ryding E, *et al.* Evaluation of malignancy in ring enhancing brain lesions on CT by thallium-201 SPECT. J Neurol Neurosurg Psychiatry 1997; 63: 569–74. doi:10.1136/jnnp.63.5.569.
[25] Schwartz RB, Carvalho PA, Alexander E, 3rd. Loeffler JS, Folkerth R, Holman BL. Radiation necrosis vs high-grade recurrent glioma: differentiation by using dual-isotope SPECT with ^{201}TI and ^{99m}Tc-HMPAO. AJNR Am J Neuroradiol 1991; 12: 1187–92.
[26] Carvalho PA, Schwartz RB, Alexander E, 3rd. *et al.* Detection of recurrent gliomas with quantitative thallium-201/technetium-99m HMPAO single-photon emission computerized tomography. J Neurosurg 1992; 77: 565–70. doi: 10.3171/jns.1992.77.4.0565.
[27] Black KL, Emerick T, Hoh C, Hawkins RA, Mazziotta J, Becker DP. Thallium-201 SPECT and positron emission tomography equal predictors of glioma grade and recurrence. Neurol Res 1994; 16: 93–6.
[28] Slizofski WJ, Krishna L, Katsetos CD, *et al.* Thallium imaging for brain tumors with results measured by a semiquantitative index and correlated with histopathology. Cancer 1994; 74: 3190–7. doi:10.1002/1097-0142(19941215)74:12<3190::AID-CNCR2820741218>3.0.CO;2-#.
[29] Serizawa T, Saeki N, Higuchi Y, *et al.* Diagnostic value of thallium-201 chloride single-photon emission computerized tomography in differentiating tumor recurrence from radiation injury after gamma knife surgery for metastatic brain tumors. J Neurosurg 2005; 102(Suppl), 266–71.
[30] Gomez-Rio M, Rodriguez-Fernandez A, Ramos-Font C, Lopez-Ramirez E, Llamas-Elvira JM. Diagnostic accuracy of ^{201}thallium-SPECT and ^{18}F-FDG-PET in the clinical assessment of glioma recurrence. Eur J Nucl Med Mol Imaging 2008; 35: 966–75. doi:10.1007/s00259-007-0661-5.
[31] Iida G, Ogawa K, Ishiuchi S, *et al.* Clinical significance of thallium-201 SPECT after postoperative radiotherapy in patients with glioblastoma multiforme. J Neurooncol 2011; 103: 297–305. doi:10.1007/s11060-010-0373-8.
[32] Vertosick FT, Jr. Selker RG, Grossman SJ, Joyce JM. Correlation of thallium-201 single photon emission computed tomography and survival after treatment failure in patients with glioblastoma multiforme. Neurosurgery 1994; 34: 396–401. doi:10.1227/00006123-199403000-00002.
[33] Caresia AP, Castell-Conesa J, Negre M, *et al.* Thallium-201 SPECT assessment in the detection of recurrences of treated gliomas and ependymomas. Clin Transl Oncol 2006; 8: 750–4. doi:10.1007/s12094-006-0122-9.
[34] Ortega-Lozano SJ, del Valle-Torres DM, Gomez-Rio M, Llamas-Elvira JM. Thallium-201 SPECT in brain gliomas: quantitative assessment in differential diagnosis between tumor recurrence and radionecrosis. Clin Nucl Med 2009; 34: 503–5. doi:10.1097/RLU.0b013e3181abb604.
[35] Vos MJ, Berkhof J, Postma TJ, Hoekstra OS, Barkhof F, Heimans JJ. Thallium-201 SPECT: the optimal prediction of response in glioma therapy. Eur J Nucl Med Mol Imaging 2006; 33: 222–7. doi:10.1007/s00259-005-1883-z.
[36] Comte F, Bauchet L, Rigau V, *et al.* Correlation of preoperative thallium SPECT with histological grading and overall survival in adult gliomas. Nucl Med Commun 2006; 27: 137–42. doi:10.1097/01.mnm.0000191855.19327.af.
[37] Vos MJ, Berkhof J, Hoekstra OS, *et al.* MRI and thallium-201 SPECT in the prediction of survival in glioma. Neuroradiology 2011doi: 10.1007/s00234-011-0908-5.
[38] Vos MJ, Hoekstra OS, Barkhof F, *et al.* Thallium-201 single-photon emission computed tomography as an early predictor of outcome in recurrent glioma. J Clin Oncol 2003; 21: 3559–65. doi:10.1200/JCO.2003.01.001.
[39] Datta NR, Pasricha R, Gambhir S, Phadke RV, Prasad SN. Postoperative residual tumour imaged by contrast-enhanced computed tomography and ^{201}Tl single photon emission tomography: can they predict progression-free survival in high-grade gliomas? Clin Oncol (R Coll Radiol) 2004; 16: 494–500. doi:10.1016/j.clon.2004.06.021.
[40] Semba T, Sugawara Y, Ochi T, Fujii T, Mochizuki T, Ohnishi T. Thallium-201 SPECT in prognostic assessment of malignant gliomas treated with postoperative radiotherapy. Ann Nucl Med 2006; 20: 287–94. doi:10.1007/BF02984645.
[41] Byrne TN. Imaging of gliomas. Semin Oncol 1994; 21: 162–71.
[42] Kumar AJ, Leeds NE, Fuller GN, *et al.* Malignant gliomas: MR imaging spectrum of radiation therapy-and chemotherapy-induced necrosis of the brain after treatment. Radiology 2000; 217: 377–84.
[43] Vos MJ, Uitdehaag BMJ, Barkhof F, *et al.* Interobserver variability in the radiological assessment of response to chemotherapy in glioma. Neurology 2003; 60: 826–30.
[44] Weckesser M, Matheja P, Rickert CH, *et al.* High uptake of *L*-3-[^{123}I]iodo-alpha-methyl tyrosine in pilocytic astrocytomas. Eur J Nucl Med 2001; 28: 273–81. doi:10.1007/s002590000462.
[45] Kallen K, Heiling M, Andersson AM, Brun A, Holtas S, Ryding E. Preoperative grading of glioma malignancy with thallium-201 single-photon emission CT: comparison with conventional CT. Am J Neuroradiol 1996; 17: 925–32.
[46] Lam W, Chan K, Wong W, Poon W, Metreweli C. Pre-operative grading of intracranial glioma. Comparison of MR-determined cerebral blood volume maps with thallium-201 SPECT. Acta Radiol 2001; 42: 548–54. doi:10.1034/j.1600-0455.2001.420603.x.
[47] Thie JA. Understanding the standardized uptake value, its methods, and implications for usage. J Nucl Med 2004; 45: 1431–4.
[48] Beauregard J-M, Hofman MS, Pereira JM, Eu P, Hicks RJ. Quantitative ^{177}Lu SPECT (QSPECT) imaging using a commercially available SPECT/CT system. Cancer Imaging 2011; 11: 56–66. doi:10.1102/1470-7330.2011.0012.
[49] Bailey D, Roach P, Bailey E, Hewlett J, Keijzers R. Development of a cost-effective modular SPECT/CT scanner. Eur J Nucl Med Mol Imaging 2007; 34: 1415–26. doi:10.1007/s00259-006-0364-3.
[50] Meikle SR, Hutton BF, Bailey DL. A transmission-dependent method for scatter correction in SPECT. J Nucl Med 1994; 35: 360–7.
[51] Brown S, Bailey DL, Willowson K, Baldock CA. Investigation of the relationship between linear attenuation coefficients and CT

Hounsfield units using radionuclides for SPECT. Appl Radiat Isot 2008; 66: 1206–12. doi:10.1016/j.apradiso.2008.01.002.

[52] Axelsson B, Msaki P, Israelsson A. Subtraction of Compton-scattered photons in single-photon emission computerized tomography. J Nucl Med 1984; 25: 490–4.

[53] Chang LT. A method for attenuation correction in radionuclide computed tomography. IEEE Trans Nucl Sci 1978; 25: 638–43. doi:10.1109/TNS.1978.4329385.

[54] Boucek JA, Francis RJ, Jones CG, Khan N, Turlach BA, Green AJ. Assessment of tumour response with ^{18}F-fluorodeoxyglucose positron emission tomography using three-dimensional measures compared to SUVmax – a phantom study. Phys Med Biol 2008; 53: 4213–30. doi:10.1088/0031-9155/53/16/001.

[55] Vertosick FTJ, Selker RG, Grossman SL, Joyce JM. Correlation of thallium-201 single photon emission computed tomography and survival after treatment failure in patients with glioblastoma multiforme. Neurosurgery 1994; 34: 396–401. doi:10.1227/00006123-199403000-00002.